Hindawi Publishing Corporation
Journal of Nanotechnology
Volume 2012, Article ID 917320, 12 pages
doi:10.1155/2012/917320

Review Article

One-Dimensional SnO_2 Nanostructures: Synthesis and Applications

Jun Pan,[1,2] Hao Shen,[1] and Sanjay Mathur[1]

[1] *Institute of Inorganic and Materials Chemistry, University of Cologne, 50939 Cologne, Germany*
[2] *Division of Physics and Applied Physics, School of Physical and Mathematical Sciences, Nanyang Technological University, Singapore 637371*

Correspondence should be addressed to Jun Pan, jun.pan@hotmail.com

Received 11 May 2011; Accepted 10 June 2011

Academic Editor: Guozhen Shen

Nanoscale semiconducting materials such as quantum dots (0-dimensional) and one-dimensional (1D) structures, like nanowires, nanobelts, and nanotubes, have gained tremendous attention within the past decade. Among the variety of 1D nanostructures, tin oxide (SnO_2) semiconducting nanostructures are particularly interesting because of their promising applications in optoelectronic and electronic devices due to both good conductivity and transparence in the visible region. This article provides a comprehensive review of the recent research activities that focus on the rational synthesis and unique applications of 1D SnO_2 nanostructures and their optical and electrical properties. We begin with the rational design and synthesis of 1D SnO_2 nanostructures, such as nanotubes, nanowires, nanobelts, and some heterogeneous nanostructures, and then highlight a range of applications (e.g., gas sensor, lithium-ion batteries, and nanophotonics) associated with them. Finally, the review is concluded with some perspectives with respect to future research on 1D SnO_2 nanostructures.

1. Introduction

One-dimensional (1D) nanoscale materials, such as nanotubes, nanowires, and nanobelts, have attracted significant attention due to their unique size- and dimensionality-dependent electrical, optical, chemical, and mechanical properties and promising applications as interconnection and functional components in designing nano-sized electronic and optical devices [1, 2]. 1D semiconductor nanostructures represent an important and broad class of nanoscale wire-like structure, which can be rationally and predictably synthesized in single crystalline form with controlled chemical composition, diameter, length, and doping level with high precision. The availability of nanostructures has enabled a wide-range of proto-type devices and integration strategies [3, 4].

It is well known that materials behave differently at the nanoscale than their bulk counterparts. Low-dimensional nanoscale materials, with their large surface areas and possible quantum confinement effects, exhibit superior mechanical, thermal, chemical, electrical, and optical properties distinct from their bulk counterparts. The manipulation of well-controlled precise dimensions, crystallinity, and composition of 1D nanostructures gives rise to unique properties, thus enabling a variety of applications that would not be possible with materials with bulk dimensionality. Doubtlessly, a thorough understanding of the fundamental properties of the 1D nanostructures system is indisputably the prerequisite of research and development towards practical applications [5].

As a n-type direct wide-band semiconductor (E_g = 3.6 eV at 300 K), SnO_2 is transparent in the visible light region and useful as optoelectronic devices [6], catalyst supports [7], transparent conducting electrodes [8], antireflective coatings [9], and a proto-type material for metal oxide sensors [10]. One-dimensional tin oxide nanostructures have been synthesized by a variety of techniques, including vapor transport [11], carbothermal reduction [12], laser ablation of pure tin in an oxidizing Ar/O_2 atmosphere [13], oxidation of electrodeposited tin wires [14], oxidation of tin vapors at elevated temperatures [15], solvothermal synthesis [16], and electrospinning [17], and so forth, Our group reported a molecule-based chemical vapor deposition (MB-CVD) to synthesize 1D SnO_2 nanowires [18, 19], nanowire arrays [20, 21], and heterostructures [22] by the decomposition

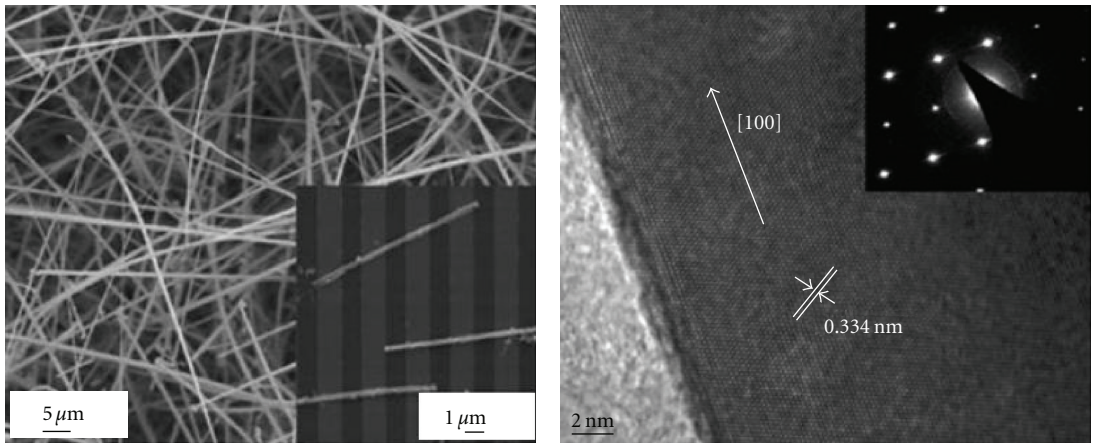

(a) (b)

Figure 1: SEM image and of high-resolution TEM image with the corresponding SAED pattern of SnO_2 nanowires.

of a single-molecular precursor $[Sn(O^tBu)_4]$ containing preformed Sn-O bonds on gold nanoparticles, on a Si, Al_2O_3, and TiO_2 substrates via the well-known vapor-liquid-solid (VLS) growth mechanism. Meanwhile it is precisely controlled over chemical composition, morphology, and deposition rate.

This article will provide a helpful review of the state-of-the-art research activities focused on synthesis and devices of 1D SnO_2 nanostructures. The first section introduces typical 1D nanostructures obtained on SnO_2, including nanowires, nanotubes, nanobelts, and some special nanostructures. Next, some important electronic and optoelectronic devices built on 1D SnO_2 nanostructures are presented, which include gas sensor, lithium-ion batteries, and nanophotonics. This review will then conclude with some perspectives and outlook on the future developments in the 1D SnO_2 nanostructures and related research areas.

2. Typical 1D SnO_2 Nanostructures

2.1. Nanowires. SnO_2 nanowires have been synthesized by several physical and chemical methods, for example, vapor-solid (VS) synthesis by SnO evaporation under pulsed flow conditions led to the formation segmented wires [23]. In addition, thermal evaporation of SnO or SnO_2 was also used to the formation of nanowires in high quantity [24]. Further, SnO_2 nanowires have been obtained by self-catalyzed growth mechanism via carbothermal synthesis [25], the laser ablation of pure tin in oxidising Ar/O_2 atmosphere [13], and oxidation of electrodeposited tin wires within structure directing AAO membranes [26] or through oxidation of tin vapours at elevated temperatures [15]. The catalyst-assisted molecule-based CVD growth is a generic approach towards controlled synthesis of metal oxide nanostructures and had been demonstrated for SnO_2, as shown in Figure 1. It is revealed that the average radial dimension of the SnO_2 wires is approximately 0.9–1.1 μm. The indexing of the SAED pattern shows that the SnO_2 nanowires grow along the [100] direction with an interplanar spacing of 0.334 nm, which corresponds to the {110} plane of SnO_2 in the rutile phase [18]. Large surfaces covered with tin oxide nanorods could be achieved by an aqueous approach controlling ionic strength and pH of precursor solutions [27].

2.2. Nanotubes. Considerable attention has also been paid to semiconducting nanotubes due to high surface-to-volume ratios compared with their solid wire counterparts since the first report of carbon nanotubes by Iijima in 1991 [28]. Nanotubes are often obtained for materials with layered or pseudolayered structures [29]. For the preparation of SnO_2 tubular structures, the template-assisted approach has been proven to be an effective route, which generally involves the use of removable templates, such as preobtained nanorods [30], cellular fibers [31], porous membranes [32], and carbon nanotubes (CNTs) [33]. However, the morphologies of the tubular structures are rather limited due to the difficulty in fabricating templates with diverse morphologies. Recently, 1D silica mesostructures are used as sacrificial templates to synthesize SnO_2 nanotubes with preserved morphologies via a simple hydrothermal route (Figure 2(a)), resulting in the formation of well-defined SnO_2 nanotubes with different lengths and unique helical SnO_2 nanotubes with a wealth of conformations (Figures 2(b) and 2(c)) [34]. In addition, SnO_2 nanotubes with controlled diameter and length were synthesized using an electrochemical method at room temperature. The length and wall thickness of the nanotubes increased monotonically with the deposition time, and the diameter of the nanotubes was altered by varying the pore size of the scaffolds [35].

2.3. Nanobelts. Nanobelts (or nanoribbons), an independent family in the realm of 1D nanomaterials, are regarded as an ideal system to fully understand dimensionally confined transport phenomena and may act as valuable units to construct nanodevices owing to their well-defined geometry [36]. SnO_2 nanobelts have been successfully synthesized by thermal evaporation of different source materials. Structurally perfect and uniform single crystalline SnO_2

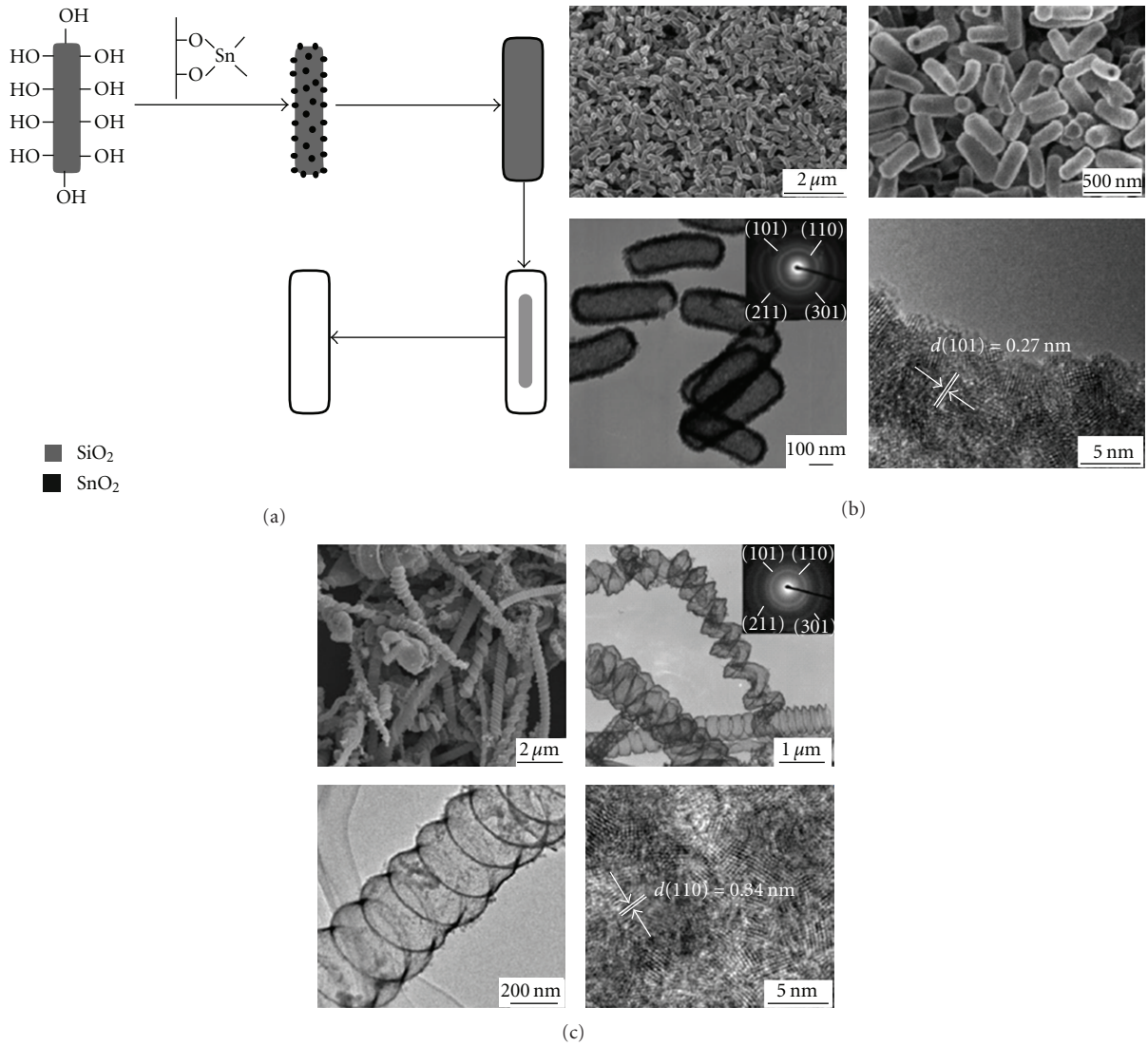

FIGURE 2: (a) Schematic illustration of a tentative mechanism for the template-directed formation of SnO_2 nanotubes. SEM and TEM images of (b) short and (c) helical SnO_2 nanotubes.

nanoribbons, with widths of 30–200 nm, width-to-thickness ration of 5–10, and length of several hundred micrometers to a few millimeters, were synthesized by simple thermal evaporation of SnO_2 or SnO powder at high temperatures. It is worth to notice that wire-like nanostructures can be observed in the first stage of growth process due to the presence of strain. The profile of the fringes implies that the geometrical shape of wire-like nanostructures is likely to be a ribbon [37]. SnO_2 nanobelts also were synthesized by mixture of Sn foil and SnO powders with the same growth mechanism [24]. A simple rapid oxidation of elemental tin was proposed for large-scale production of SnO_2 nanoribbons. The width of the nanostructure was sensitive to the reaction temperature. When the growth temperature was increased to 1350°C, the diameter range of these nanostructures increased markedly to 50–350 nm (Figure 3(b)) compared to the wire-like nanostructures grown at 1080°C (Figure 3(a)). The lengths of the nanoribbons were up to several hundreds of micrometers, and the typical width and thickness were in the range of 30–150 nm and 10–30 nm (Figure 3(c)), respectively. The as-synthesized SnO_2 nanoribbons appeared to be single crystalline and exhibited [110] and [203] growth directions (Figures 3(d)–3(e)) [38]. Recently, {101} surfaces of zigzag SnO_2 nanobelts have been synthesized by a VS process, which are reduced surfaces terminated by Sn atoms and the Sn terminated surface is a nonpolar surface. As both reduced SnO and stoichiometric SnO_2 (101) surfaces are neutral terminations, the polar surface model is no more suitable for the (101) type surface of rutile SnO_2 nanobelts [39].

2.4. Other SnO_2 1D Nanostructures. Synthesis and assembly of SnO_2 1D nanostructures with special morphologies, shapes, and compositions have attracted great interests very recently because they process unique properties and functionalities that are not accessible in the single-component materials, due to the combination of material classes such

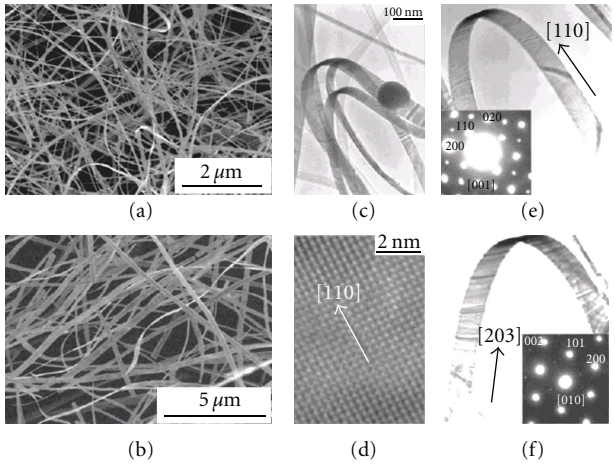

Figure 3: SEM images of SnO_2 (a) wire-like nanostructures and (b) nanoribbons, and TEM images (c)–(f) of SnO_2 nanoribbons.

as metals, metal oxides, semiconductors, and polymers. They may also be used to fabricate special electronic and optoelectronic devices which cannot be fulfilled using simple 1D nanostructures [40, 41]. Branched 1D SnO_2-V_2O_5 heterostructures were fabricated by growing vanadium oxide nanostructures on as-grown SnO_2 backbones (Figure 4(a)). HR-TEM images of the SnO_2-V_2O_5 interface revealed a strong alignment of the two different crystal lattices, resulting in a heteroepitaxial growth of vanadium oxide on tin oxide. The single-crystalline nature and growth direction of the V_2O_5 were indexed to be ⟨111⟩ (Figure 4(b)) [20]. Hierarchical nanostructures with SnO_2 backbones and ZnO branches are successfully prepared in a large scale by combining the vapor transport and deposition process (for SnO_2 nanowires) and a hydrothermal growth (for ZnO). The ZnO nanorods grow epitaxially on the SnO_2 nanowire side faces mainly with a four-fold symmetry. The number density and morphology of secondary ZnO nanostructure can be tuned by adjusting the baking condition, such as the salt concentration, reaction time, and additives [42]. In addition, SnO_2 nanobelt/CdS nanoparticle core/shell heterostructures are successfully prepared via a simple and efficient sonochemical approach. The CdS nanoparticles are nearly spherical in shape and have typical sizes in the range of 10–20 nm. The measured spacing of the crystallographic planes is 0.315 nm, which corresponds to the {101} lattice plane of the hexagonal structured CdS crystal [43].

3. Applications of 1D SnO_2 Nanostructures

As an important group of wide-band gap semiconductors with tunable conductivity and high transparency, 1D SnO_2 nanostructures have been used to fabricate nanoscale gas sensor, electronic and optoelectronic devices.

3.1. Gas Sensor. Gas sensing using nanomaterials is an attractive, versatile application for important molecule species, environmental and security-checking purposes [44, 45].

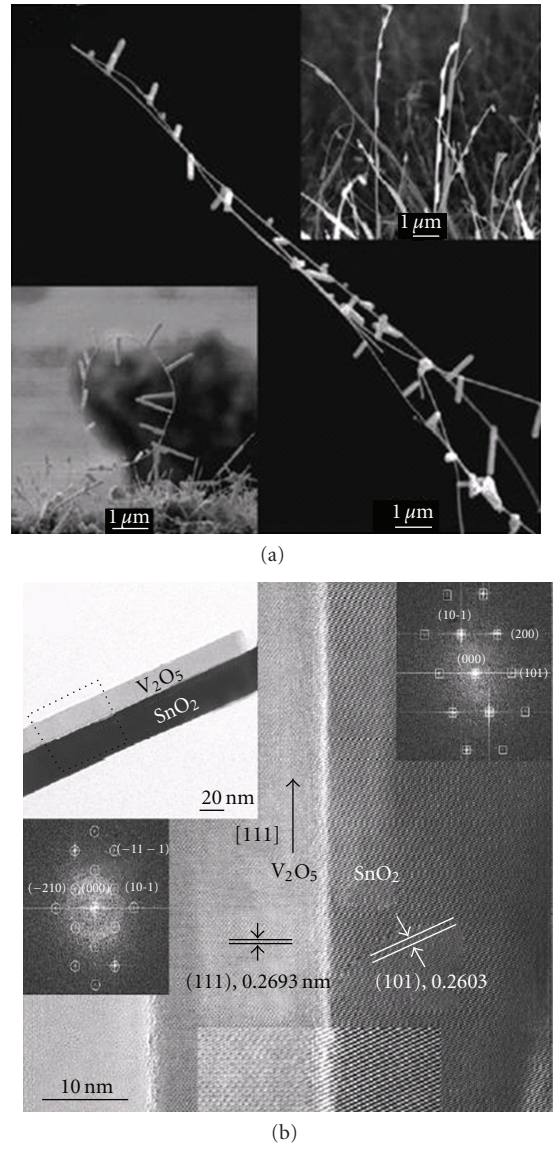

Figure 4: SEM and TEM images of SnO_2-V_2O_5 heterostructures.

The advantages of using 1D nanostructures for chemical sensing are diverse. With a large surface-to-volume ratio and a Debye length comparable to the nanowire radius, the electronic property of the nanowire is strongly influenced by surface processes, yielding superior sensitivity than their thin film counterpart. The sensing mechanism of metal oxides is mainly governed by the fact that the oxygen vacancies on the oxide surfaces are electrically and chemically active, therefore, the conductivity (or resistivity) of oxide nanomaterials is strongly affected by the adsorbed molecules. SnO_2 is n-type semiconductor with oxygen deficiency. The lattice oxygen is evaporated in the form of gas, which makes the doubly ionized oxygen vacancy and electrons. If tin dioxide is heated at 300–400°C, the oxygen in the atmosphere is adsorbed at the surface of SnO_2 with the negative charge. Because electron is provided from the surface of crystal, the surface of tin oxide becomes an electron depletion layer.

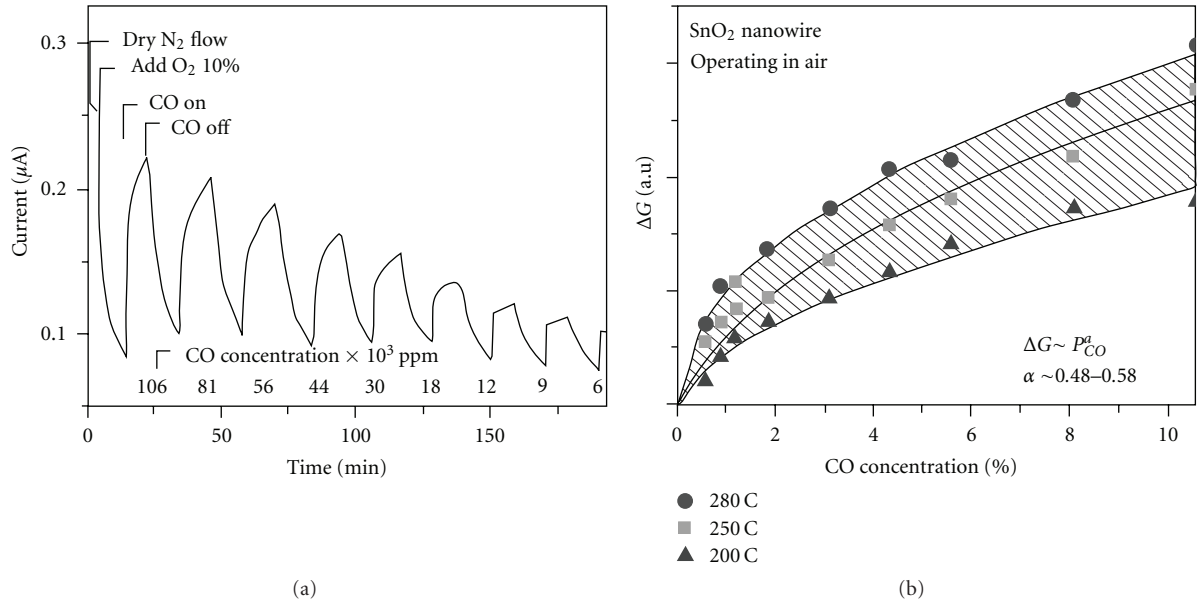

FIGURE 5: (a) Response of the SnO_2 nanowires towards CO pulses. (b) Change in conductance of individual SnO_2 nanowires as a function of CO concentration at three temperatures.

This means the formation of potential barrier near the grain boundary. If CO is present in the atmosphere, the CO oxidizes into CO_2 with the reaction of adsorbed oxygen and remaining electron returns to the SnO_2 crystal. This increases the electrical conductivity to a great extent. So, we can detect CO by measuring the remarkable resistance decrease upon CO reaction. Generally speaking, the reduction in resistance occurs mainly at the surface and can be explained by the reduction of potential barrier [46].

The first SnO_2 nanobelt chemical sensor was made on an alumina substrate by dispersing SnO_2 nanobelts atop prefabricated platinum interdigitated electrodes on a substrate. The sensor was employed to detect CO and NO_2 for environmental polluting species and ethanol for breath analysis. A single-SnO_2-nanobelt sensor integrated with microheaters to sense dimethyl methylphosphonate (DMMP) was fabricated. The conductance of the SnO_2 nanobelt sensor was reduced by 5% when the sensor was exposed to 78 ppb of DMMP [47]. It was also reported that light photoactivates molecule absorption and desorption as an alternative way to the use of temperature. An explosive environment is the typical application where the use of heated sensors is not favorable. The strong photoconducting response of individual single-crystalline SnO_2 nanoribbons makes it possible to achieve equally favorable adsorption-desorption behavior at room temperature by illuminating the devices with a ultraviolet (UV) light of energy near the SnO_2 bandgap. The active desorption process is thus photoinduced molecular desorption [48]. Kolmakov et al. realized an array of parallel nanowires of SnO_2 by using self organized highly ordered porous alumina templates. Conductance measurements were performed on isolated individual nanowires with vapor-deposited Ti/Au microcontacts. They analyzed the behavior of nanowire in N_2 and N_2 + 10% O_2. CO reacts with preadsorbed oxygen species on SnO_2 to form carbon monoxide thus donating few electrons back into the bulk resulting in an increased conductivity, which depends monotonically on the gas phase partial pressure of CO (Figure 5) [14]. Single SnO_2 metal oxide nanowires are used at the nanoscale level as individual monocrystal for the electrical transduction of the gas interaction with these sensing materials. Electrical contact characteristics and resistance variations under different gas ambient are analyzed from two- and four-probe measurements of individual nanowires. CO and humidity behaviors are reported for single SnO_2 nanowires with CO detection threshold smaller than 5 ppm and measurement instability lower than 4% (Figure 6) [49]. A technical approach to fabricate practical devices by coupling a single-crystal SnO_2 nanowire sensing element with a microhotplate gas sensor platform was also presented [50].

In order to tune the sensitivity and selectivity of SnO_2 nanowires-based sensors, many techniques have been explored. The addition of a small amount of noble metals such as Au, Pd, Pt, and Ag and Ni speeds up surface reactions and improves selectivity towards target gas species [51]. Kolmakov examined the influence of the surface sensitization with catalyst particles of Ni/NiO and Pd [52]. Wan reported the use of Sb doping to tailor the resistivity of SnO_2 nanowires deposited by thermal evaporation process starting from a mixture of Sn and Sb powders in the ratio 10 : 1 [53]. Meanwhile, Pan et al. modified SnO_2 nanowires by Ar/O_2 plasma treatment through preferential etching of the lattice oxygen atoms, which produced nonstoichiometric surface compositions that imparted a many-fold higher sensitivity toward gas absorption on such surfaces (Figure 7) [54].

3.2. Anode Materials for Lithium-Ion Batteries. Rechargeable lithium-ion batteries (LIBs) have been recognized as

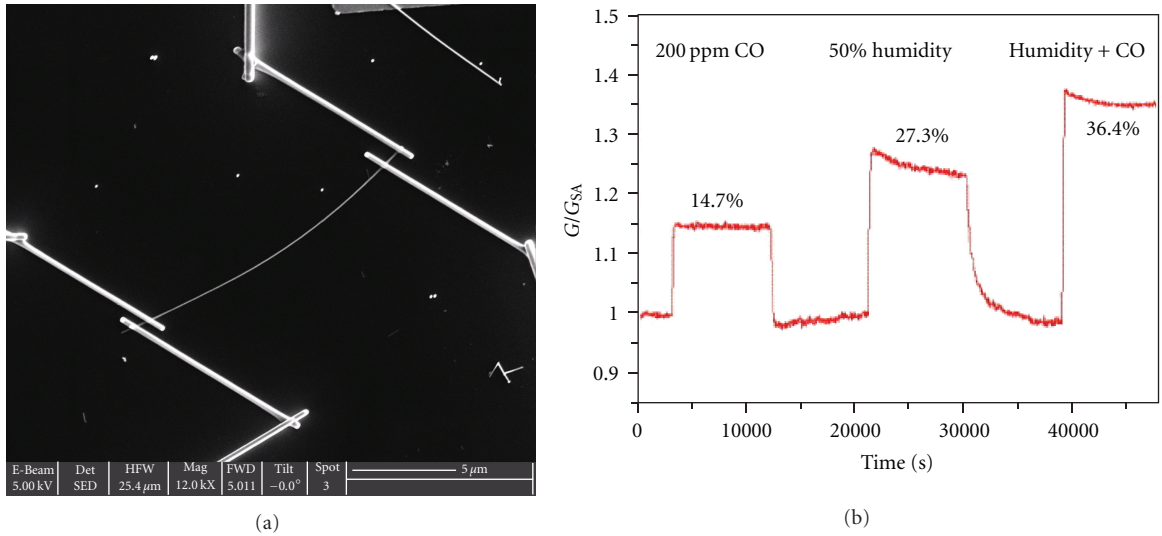

Figure 6: (a) A single SnO_2 nanowires contacted in a 4-probes configuration. (b) Comparison between the simultaneous detection of 200 ppm of CO and 50% of RH.

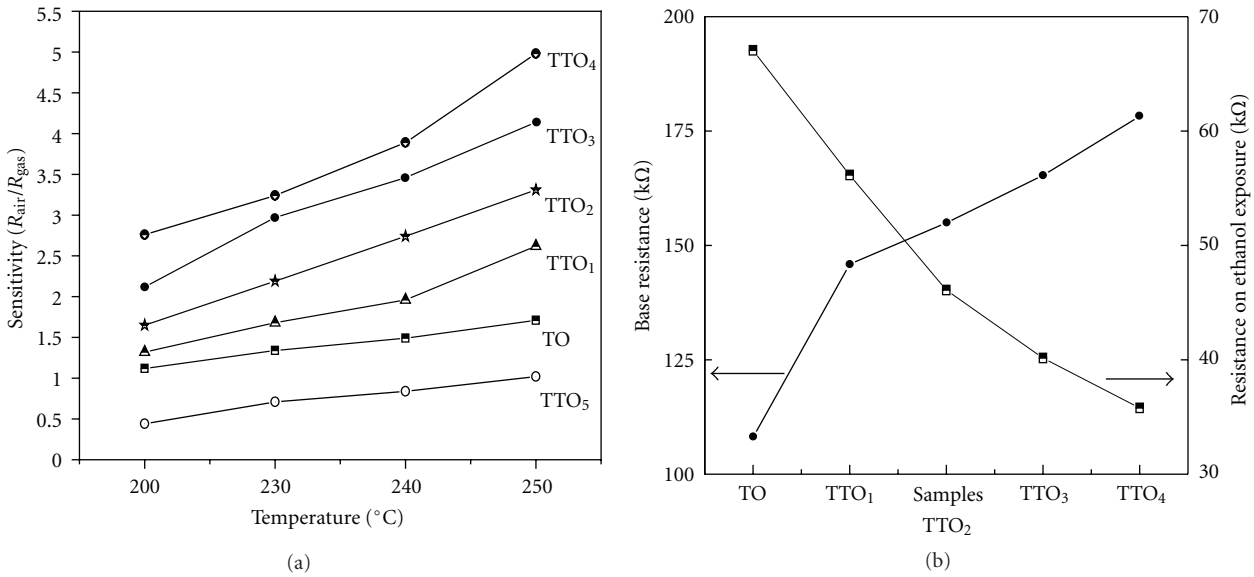

Figure 7: (a) Temperature-dependent sensing response curves and (b) base and sensing resistances dependency to the power of plasma treatment.

an attractive power source for popular mobile devices. At present, LIBs are efficient, light-weight, and rechargeable power sources for consumer electronics such as laptop computers, digital cameras, and mobile phones. Moreover, they have been extensively studied for use as power supplies of electric vehicles (EVs) and hybrid electric vehicles (HEVs), which require high energy and power densities [55].

As a promising anode material for LIBs, tin-based material has attracted growing attention owing to the extraordinary electrochemical behavior, such that the initial irreversible capacity induced by Li_2O formation, and the abrupt capacity fading caused by volume variation could be effectively reduced when in nanoscale form, the high theoretical capacity (992 $mAhg^{-1}$) and the higher operating voltage comparing to traditional carbonaceous anode active materials [56, 57]. The self-catalytically grown SnO_2 nanowires could provide more reaction sites on the surface and enhance the charge transfer in the electrochemical reactions. Moreover, Sn particles at the tips of nanowires also contributed to the Li^+ storage and prevented the capacity loss that is induced by the existing metal catalysts. SnO_2 nanowires showed an initial Coulombic efficiency of approximately 46.91% and improved cyclic performance and a higher reversible specific capacity of over 300 $mAhg^{-1}$ up to the 50th cycle as shown in Figure 8 [58]. In addition, SnO_2 nanowire

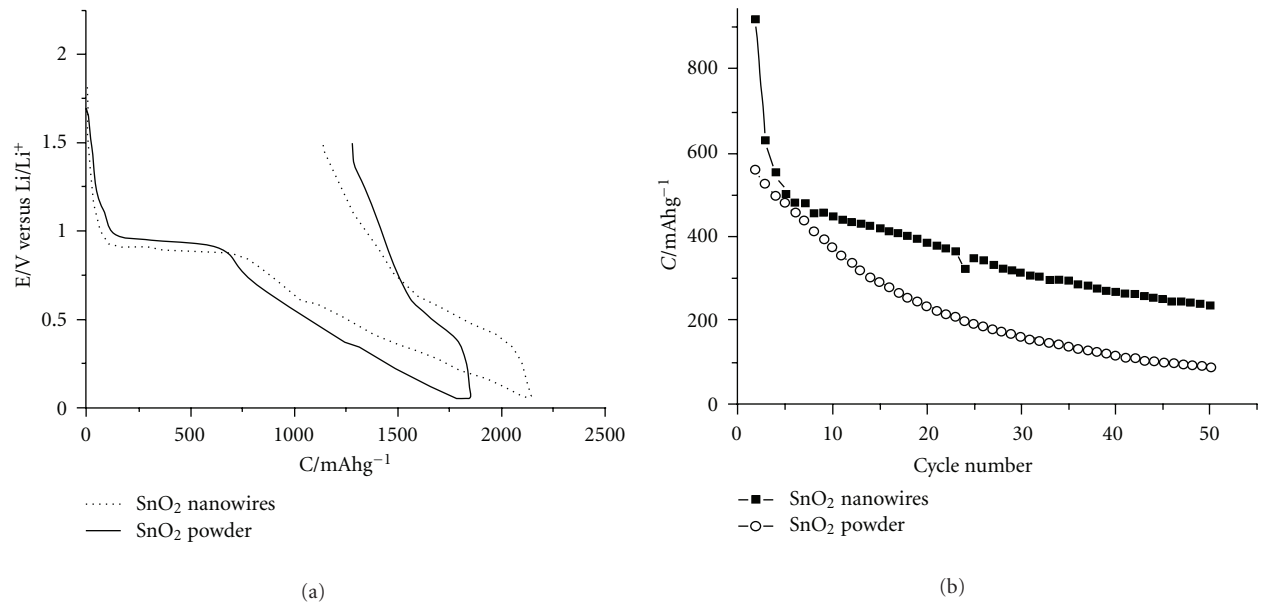

Figure 8: (a) The voltage profile for the first cycle between 0.05 V and 1.5 V compared with pure SnO_2 powder. (b) The cyclic performance from the second cycle to the 50th cycle of SnO_2 nanowires and pure SnO_2 powder.

electrode without any buffer layer was used as rechargeable LIBs and exhibited superior electrochemical performance stable cycling behaviors and delivered a high specific discharge capacity of 510 $mAhg^{-1}$, even at the 50th cycle [59].

SnO_2 nanorod arrays represent an excellent geometry because they can offer direct channels for efficient electron transport. SnO_2 nanorod array electrodes can be produced in a one-pot template-free alkaline hydrothermal process. The array electrode showed good performance as a LIB anode in properties such as capacity retention (580 $mAhg^{-1}$ after 100 cycles at 0.1 C) and rate capability (stable 350 $mAhg^{-1}$ at 5 C) [60].

SnO_2-based heterostructure is a very promising strategy to achieve high-power-density and high-energy-density LIBs. A high electrochemical activity of V_2O_5 loaded on SnO_2 nanowire-based electrode showed a very-high rate capability. The thin V_2O_5 layer is beneficial for fast Li^+ intercalation/deintercalation, while the SnO_2 core nanowire provides a fast path for electron transportation and also increases the electrochemical utilization of V_2O_5. SnO_2/V_2O_5 core/shell nanowires could deliver a high power density of 60 $kWkg^{-1}$ while the energy density remains as high as 282 $Whkg^{-1}$. A better rate capability was achieved at high temperature (Figure 9) [61]. Carbon-coated SnO_2 nanorod array also revealed excellent cycling stability (stable 320 $mAhg^{-1}$ at 3000 mAg^{-1}) and rate capability (585 $mAhg^{-1}$ after 50 cycles at 500 mAg^{-1}) [62].

3.3. Nanophotonics. Nanowires represent attractive building blocks for active nanophotonic devices, including light-emitting diodes (LEDs), lasers, and detectors [63, 64]. Significantly, the ability to assemble and electrically drive nanoscale sources and detector blocks could allow for fully integrated nanophotonic systems for use in applications ranging from biodetection through information processing. Nanowires of binary oxides have been employed throughout this work because of the variety of beneficial properties, including extreme mechanical flexibility and chemical stability.

SnO_2, has recently been shown to act as an excellent subwavelength waveguide because of its defect-related PL bands at 2.5 eV (green) and 2.1 eV (orange) (Figure 10) [65]. Nonresonant waveguiding (i.e., subbandgap light) in these structures can be achieved by simply focusing laser diodes on the end facet of the nanowire. SnO_2 wires have dimensions between 100 nm and 400 nm, an optimal size range to efficiently guide visible and UV wavelengths because of the high index of refraction of SnO_2 ($n > 2$). Optical linkages between active nanowires (GaN and ZnO) and passive nanowires (SnO_2) can be formed via tangential evanescent coupling (Figure 11). It has been shown that a staggered side-by-side configuration, in which the active and passive elements interact over a few microns, outperforms bridged, or direct end-to-end coupling. Weaker coupling is achieved by staggering structures with a thin air gap (several hundred nanometers) between them, allowing communication via tunneling of evanescent waves [66]. With further integration, it should be possible to create more functional geometries, such as branched optical hubs and Mach-Zehnder interferometers (optical modulators) that use the electro-optic effect for phase shifting. The integration of high-frequency electrically driven lasers with passive nanowire waveguides is the next step toward effectively transducing and routing packets of optical information within an optical computer

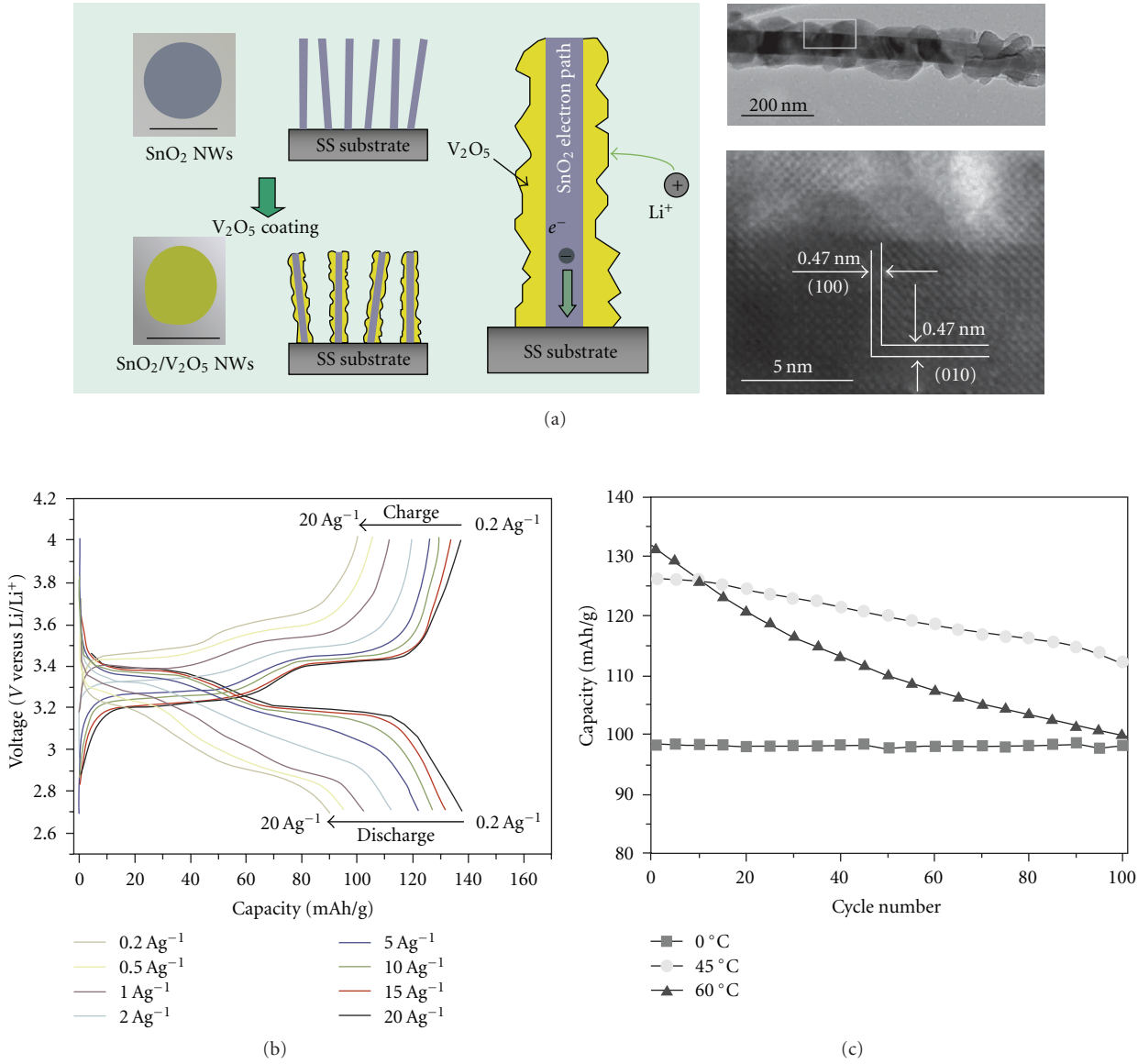

Figure 9: (a) Schematic diagram showing the strategy for coating V_2O_5 on SnO_2 nanowires, and typical TEM images of a single SnO_2/V_2O_5 core/shell nanowires, (b) the galvanostatic charge/discharge curves at different current densities, and (c) the cycling performance at different temperatures of the SnO_2/V_2O_5 core/shell nanowires electrode tested.

or communication device [67]. However, the goal of room temperature, electrically driven nanolasers, remains an active area of current research.

4. Summary and Perspective

In summary, we provide a comprehensive review of the state-of-the-art research activities focused on rational synthesis (e.g., nanowires, nanobelts, nanotubes, and heterostructures) and potential applications (e.g., gas sensor, lithium-ion batteries, and nanophotonics) of 1D SnO_2 nanostructures. The fascinating achievements, till now, towards the device applications of 1D SnO_2 nanostructures should inspire more and more research efforts to address the remaining challenges in this interesting field in the future.

Controlled manipulation of matter at the nanoscale will lead to fascinating and novel behavior and also impact device properties. The ability to rationally control key 1D SnO_2 nanostructures parameters during growth, fabricate intra-NW heterostructures with well defined [68], and atomically abrupt crystalline interfaces should further increase the versatility of 1D SnO_2 nanostructure-based electronic and photonic devices and also reduce the load for subsequent assembly processes.

Such a synthetic control will be extremely useful for creating precisely defined systems to investigate the effects of quantum confinement on electronic and optical properties

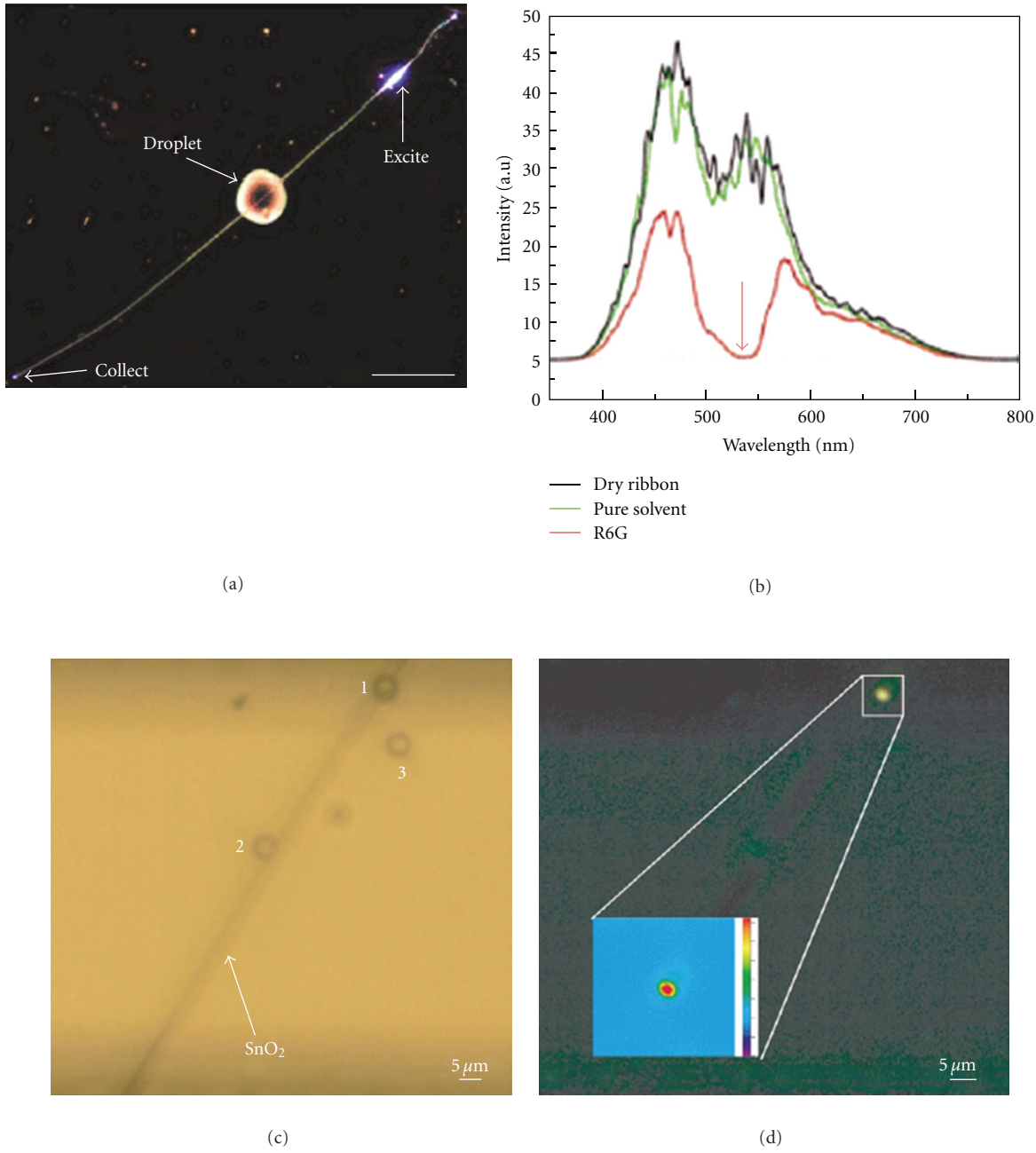

FIGURE 10: Demonstration of absorption and fluorescence schemes using individual SnO_2 nanoribbon waveguides. (a) Dark-field photoluminescence image of the absorption scheme showing an analyte centered in the middle of the ribbon and the labeled excitation and collection locations. (b) Spectra recorded after the SnO_2 defect emission traversed through the ribbon in air (black), pure glycol (green), and 1 mM dye-loaded glycol (red). (c) Bright-field image of 2 μm yellow-green fluorescent polystyrene beads placed with an optical trap precisely on or near a SnO_2 nanoribbon. (d) Fluorescence image of beads after waveguiding of photoluminescence from the SnO_2 ribbon. Inset: false color expansion of bead 1 during UV excitation of the ribbon.

of nanostructures resulting from the modification of the electronic density of states and also aid in developing novel nanophotonic devices.

Looking into the future, with extensive research in nanostructures synthesis to accurately control dimension and composition, a critical understanding of the modified properties of materials at the nanoscale, and the hierarchical assembly of nanostructures with exquisite spatial control, progress will be made, and new and interesting nanosystems will create the technologies of the future.

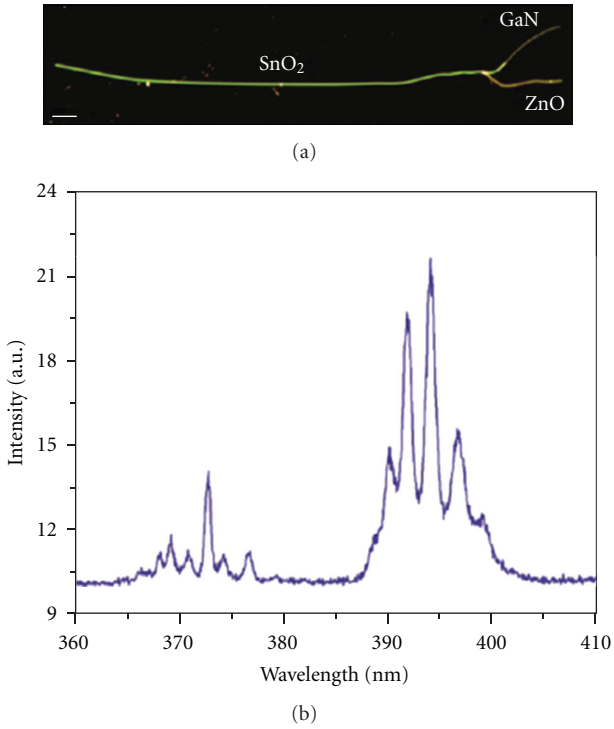

Figure 11: (a) Dark-field image illustrating the coupling of two nanowire lasers (GaN and ZnO) to a common SnO_2 nanoribbon waveguide. Scale bar = 25 μm. (b) Spectra recorded at the left terminus of the SnO_2 nanoribbon after simultaneous nanowire laser injection.

Acknowledgment

The authors graciously thank the scientists cited in this paper for their contributions to the research.

References

[1] Y. Xia, P. Yang, Y. Sun et al., "One-dimensional nanostructures: synthesis, characterization, and applications," *Advanced Materials*, vol. 15, no. 5, pp. 353–389, 2003.

[2] J. Hu, T. W. Odom, and C. M. Lieber, "Chemistry and physics in one dimension: synthesis and properties of nanowires and nanotubes," *Accounts of Chemical Research*, vol. 32, no. 5, pp. 435–445, 1999.

[3] A. P. Alivisatos, "Semiconductor clusters, nanocrystals, and quantum dots," *Science*, vol. 271, no. 5251, pp. 933–937, 1996.

[4] Y. Cui and C. M. Lieber, "Functional nanoscale electronic devices assembled using silicon nanowire building blocks," *Science*, vol. 291, no. 5505, pp. 851–853, 2001.

[5] J. Weber, R. Singhai, S. Zekri, and A. Kumar, "One-dimensional nanostructures: fabrication, characterisation and applications," *International Materials Reviews*, vol. 53, no. 4, pp. 235–255, 2008.

[6] C. Tatsuyama and S. Ichimura, "Electrical and optical-properties of gase-SnO_2 heterojunctions," *Japanese Journal of Applied Physics*, vol. 15, no. 5, pp. 843–847, 1976.

[7] W. Dazhi, W. Shulin, C. Jun, Z. Suyuan, and L. Fangqing, "Microstructure of SnO_2," *Physical Review B*, vol. 49, no. 20, pp. 14282–14285, 1994.

[8] P. G. Harrison and M. J. Willett, "The mechanism of operation of tin(IV) oxide carbon monoxide sensors," *Nature*, vol. 332, no. 6162, pp. 337–339, 1988.

[9] Y. S. He, J. C. Campbell, R. C. Murphy, M. F. Arendt, and J. S. Swinnea, "Electrical and optical characterization of Sb:SnO_2," *Journal of Materials Research*, vol. 8, no. 12, pp. 3131–3134, 1993.

[10] S. Semancik and T. B. Fryberger, "Model studies of SnO_2-based gas sensors: vacancy defects and Pd additive effects," *Sensors and Actuators B*, vol. 1, no. 1-6, pp. 97–102, 1990.

[11] Z. R. Dai, Z. W. Pan, and Z. L. Wang, "Novel nanostructures of functional oxides synthesized by thermal evaporation," *Advanced Functional Materials*, vol. 13, no. 1, pp. 9–24, 2003.

[12] S. Budak, G. X. Miao, M. Ozdemir, K. B. Chetry, and A. Gupta, "Growth and characterization of single crystalline tin oxide (SnO_2) nanowires," *Journal of Crystal Growth*, vol. 291, no. 2, pp. 405–411, 2006.

[13] Z. Liu, D. Zhang, S. Han et al., "Laser ablation synthesis and electron transport studies of tin oxide nanowires," *Advanced Materials*, vol. 15, no. 20, pp. 1754–1757, 2003.

[14] A. Kolmakov, Y. Zhang, G. Cheng, and M. Moskovits, "Detection of CO and O_2 using tin oxide nanowire sensors," *Advanced Materials*, vol. 15, no. 12, pp. 997–1000, 2003.

[15] Y. J. Ma, F. Zhou, L. Lu, and Z. Zhang, "Low-temperature transport properties of individual SnO_2 nanowires," *Solid State Communications*, vol. 130, no. 5, pp. 313–316, 2004.

[16] X. Jiang, Y. Wang, T. Herricks, and Y. Xia, "Ethylene glycol-mediated synthesis of metal oxide nanowires," *Journal of Materials Chemistry*, vol. 14, no. 4, pp. 695–703, 2004.

[17] D. Li, Y. Wang, and Y. Xia, "Electrospinning nanofibers as uniaxially aligned arrays and layer-by-layer stacked films," *Advanced Materials*, vol. 16, no. 4, pp. 361–366, 2004.

[18] S. Mathur, S. Barth, H. Shen, J. C. Pyun, and U. Werner, "Size-dependent photoconductance in SnO_2 nanowires," *Small*, vol. 1, no. 7, pp. 713–717, 2005.

[19] J. Pan, L. Xiao, H. Shen, and S. Mathur, "Mechanistic studies on chemical vapor deposition grown tin oxide nanowires," *Ceramic Engineering and Science Proceedings*, vol. 30, no. 7, pp. 9–15, 2010.

[20] S. Mathur and S. Barth, "Molecule-based chemical vapor growth of aligned SnO_2 nanowires and branched SnO_2/V_2O_5 heterostructures," *Small*, vol. 3, no. 12, pp. 2070–2075, 2007.

[21] J. Pan, H. Shen, U. Werner et al., "Heteroepitaxy of SnO_2 nanowire arrays on TiO_2 single crystals: growth patterns and tomographic studies," *Journal of Physical Chemistry C*, vol. 115, no. 31, pp. 15191–15197, 2011.

[22] J. Pan, S. Hühne, H. Shen et al., "SnO_2-TiO_2 core-shell nanowire structures: investigation on solid state reactivity and photocatalytic behaviors," *Journal of Physical Chemistry C*, vol. 115, no. 35, pp. 17265–17269, 2011.

[23] Y. Lilach, J. P. Zhang, M. Moskovits, and A. Kolmakov, "Encoding morphology in oxide nanostructures during their growth," *Nano Letters*, vol. 5, no. 10, pp. 2019–2022, 2005.

[24] Z. R. Dai, J. L. Gole, J. D. Stout, and Z. L. Wang, "Tin oxide nanowires, nanoribbons, and nanotubes," *Journal of Physical Chemistry B*, vol. 106, no. 6, pp. 1274–1279, 2002.

[25] B. Wang, Y. H. Yang, C. X. Wang, and G. W. Yang, "Nanostructures and self-catalyzed growth of SnO_2," *Journal of Applied Physics*, vol. 98, no. 7, Article ID 073520, 5 pages, 2005.

[26] M. Zheng, G. Li, X. Zhang, S. Huang, Y. Lei, and L. Zhang, "Fabrication and structural characterization of large-scale uniform SnO_2 nanowire array embedded in anodic alumina membrane," *Chemistry of Materials*, vol. 13, no. 11, pp. 3859–3861, 2001.

[27] L. Vayssieres and M. Graetzel, "Highly ordered SnO_2 nanorod arrays from controlled aqueous growth," *Angewandte Chemie International Edition*, vol. 43, no. 28, pp. 3666–3670, 2004.

[28] S. Iijima, "Helical microtubules of graphitic carbon," *Nature*, vol. 354, no. 6348, pp. 56–58, 1991.

[29] Y. Feldman, E. Wasserman, D. J. Srolovitz, and R. Tenne, "High-rate, gas-phase growth of MoS_2 nested inorganic fullerenes and nanotubes," *Science*, vol. 267, no. 5195, pp. 222–225, 1995.

[30] B. Liu and H. C. Zeng, "Salt-assisted deposition of SnO_2 on α-moO_3 nanorods and fabrication of polycrystalline SnO_2 nanotubes," *Journal of Physical Chemistry B*, vol. 108, no. 19, pp. 5867–5874, 2004.

[31] J. Huang, N. Matsunaga, K. Shimanoe, N. Yamazoe, and T. Kunitake, "Nanotubular SnO_2 templated by cellulose fibers: synthesis and gas sensing," *Chemistry of Materials*, vol. 17, no. 13, pp. 3513–3518, 2005.

[32] Y. Wang, J. Y. Lee, and H. C. Zeng, "Polycrystalline SnO_2 nanotubes prepared via infiltration casting of nanocrystallites and their electrochemical application," *Chemistry of Materials*, vol. 17, no. 15, pp. 3899–3903, 2005.

[33] Y. Jia, L. He, Z. Guo et al., "Preparation of porous tin oxide nanotubes using carbon nanotubes as templates and their gas-sensing properties," *Journal of Physical Chemistry C*, vol. 113, no. 22, pp. 9581–9587, 2009.

[34] J. Ye, H. Zhang, R. Yang, X. Li, and L. Qi, "Morphology-controlled synthesis of SnO_2 nanotubes by using 1D silica mesostructures as sacrificial templates and their applications in lithium-ion batteries," *Small*, vol. 6, no. 2, pp. 296–306, 2010.

[35] M. Lai, J. H. Lim, S. Mubeen et al., "Size-controlled electrochemical synthesis and properties of SnO_2 nanotubes," *Nanotechnology*, vol. 20, no. 18, Article ID 185602, 2009.

[36] Z. W. Pan, Z. R. Dai, and Z. L. Wang, "Nanobelts of semiconducting oxides," *Science*, vol. 291, no. 5510, pp. 1947–1949, 2001.

[37] Z. R. Dai, Z. W. Pan, and Z. L. Wang, "Ultra-long single crystalline nanoribbons of tin oxide," *Solid State Communications*, vol. 118, no. 7, pp. 351–354, 2001.

[38] J. Q. Hu, X. L. Ma, N. G. Shang et al., "Large-scale rapid oxidation synthesis of SnO_2 nanoribbons," *Journal of Physical Chemistry B*, vol. 106, no. 15, pp. 3823–3826, 2002.

[39] N. Lu, Q. Wan, and J. Zhu, "Surface structure of zigzag SnO_2 nanobelts," *Journal of Physical Chemistry Letters*, vol. 1, no. 9, pp. 1468–1471, 2010.

[40] G. Shen, D. Chen, Y. Bando, and D. Golberg, "One-dimensional (1D) nanoscale heterostructures," *Journal of Materials Science and Technology*, vol. 24, no. 4, pp. 541–549, 2008.

[41] G. Z. Shen and D. Chen, "1D hetero-nanostructures: from growth to devices," *Science of Advanced Materials*, vol. 1, no. 3, pp. 213–226, 2009.

[42] C. Cheng, B. Liu, H. Yang et al., "Hierarchical assembly of ZnO nanostructures on SnO_2 backbone nanowires: low-temperature hydrothermal preparation and optical properties," *ACS Nano*, vol. 3, no. 10, pp. 3069–3076, 2009.

[43] T. Gao and T. Wang, "Sonochemical synthesis of SnO_2 nanobelt/CdS nanoparticle core/shell heterostructures," *Chemical Communications*, vol. 10, no. 22, pp. 2558–2559, 2004.

[44] G. Shen, "Fabrication and characterization of metal oxide nanowire sensors," *Recent Patents on Nanotechnology*, vol. 2, no. 3, pp. 160–168, 2008.

[45] G. Shen, P. C. Chen, K. Ryu, and C. Zhou, "Devices and chemical sensing applications of metal oxide nanowires," *Journal of Materials Chemistry*, vol. 19, no. 7, pp. 828–839, 2009.

[46] Y. Zhang, A. Kolmakov, S. Chretien, H. Metiu, and M. Moskovits, "Control of catalytic reactions at the surface of a metal oxide nanowire by manipulating electron density inside it," *Nano Letters*, vol. 4, no. 3, pp. 403–407, 2004.

[47] C. Yu, Q. Hao, S. Saha, L. Shi, X. Kong, and Z. L. Wang, "Integration of metal oxide nanobelts with microsystems for nerve agent detection," *Applied Physics Letters*, vol. 86, no. 6, Article ID 063101, 3 pages, 2005.

[48] M. Law, H. Kind, B. Messer, F. Kim, and P. Yang, "Photochemical sensing of NO_2 with SnO_2 nanoribbon nanosensors at room temperature," *Angewandte Chemie International Edition*, vol. 41, no. 13, pp. 2405–2408, 2002.

[49] F. Hernández-Ramírez, A. Tarancón, O. Casals, J. Arbiol, A. Romano-Rodríguez, and J. R. Morante, "High response and stability in CO and humidity measures using a single SnO_2 nanowire," *Sensors and Actuators B*, vol. 121, no. 1, pp. 3–17, 2007.

[50] D. C. Meier, S. Semancik, B. Button, E. Strelcov, and A. Kolmakov, "Coupling nanowire chemiresistors with MEMS microhotplate gas sensing platforms," *Applied Physics Letters*, vol. 91, no. 6, Article ID 063118, 2007.

[51] E. Comini, G. Faglia, G. Sberveglieri, Z. Pan, and Z. L. Wang, "Stable and highly sensitive gas sensors based on semiconducting oxide nanobelts," *Applied Physics Letters*, vol. 81, no. 10, pp. 1869–1871, 2002.

[52] A. Kolmakov, "The effect of morphology and surface doping on sensitization of quasi-1D metal oxide nanowire gas sensors," in *Nanomaterial Synthesis and Integration for Sensors, Electronics, Photonics, and Electro-Optics*, vol. 6370 of *Proceedings of SPIE*, pp. U137–U144, Boston, Mass, USA, 2006.

[53] Q. Wan and T. H. Wang, "Single-crystalline Sb-doped SnO_2 nanowires: synthesis and gas sensor application," *Chemical Communications*, no. 30, pp. 3841–3843, 2005.

[54] J. Pan, R. Ganesan, H. Shen, and S. Mathur, "Plasma-modified SnO_2 nanowires for enhanced gas sensing," *Journal of Physical Chemistry C*, vol. 114, no. 18, pp. 8245–8250, 2010.

[55] J. M. Tarascon and M. Armand, "Issues and challenges facing rechargeable lithium batteries," *Nature*, vol. 414, no. 6861, pp. 359–367, 2001.

[56] J. Hassoun, S. Panero, P. Simon, P. L. Taberna, and B. Scrosati, "High-rate, long-life Ni-Sn nanostructured electrodes for lithium-ion batteries," *Advanced Materials*, vol. 19, no. 12, pp. 1632–1635, 2007.

[57] A. I. Hochbaum and P. Yang, "Semiconductor nanowires for energy conversion," *Chemical Reviews*, vol. 110, no. 1, pp. 527–546, 2010.

[58] M. S. Park, G. X. Wang, Y. M. Kang, D. Wexler, S. X. Dou, and H. K. Liu, "Preparation and electrochemical properties of SnO_2 nanowires for application in lithium-ion batteries," *Angewandte Chemie International Edition*, vol. 46, no. 5, pp. 750–753, 2007.

[59] Y. D. Ko, J. G. Kang, J. G. Park, S. Lee, and D. W. Kim, "Self-supported SnO_2 nanowire electrodes for high-power lithium-ion batteries," *Nanotechnology*, vol. 20, no. 45, Article ID 455701, 2009.

[60] J. Liu, Y. Li, X. Huang et al., "Direct growth of SnO_2 nanorod array electrodes for lithium-ion batteries," *Journal of Materials Chemistry*, vol. 19, no. 13, pp. 1859–1864, 2009.

[61] J. Yan, A. Sumboja, E. Khoo, and P. S. Lee, "V_2O_5 loaded on SnO_2 nanowires for high-rate Li Lon batteries," *Advanced Materials*, vol. 23, no. 6, pp. 746–750, 2011.

[62] X. Ji, X. Huang, J. Liu et al., "Carbon-coated SnO_2 nanorod array for lithium-ion battery anode material," *Nanoscale Research Letters*, vol. 5, no. 3, pp. 649–653, 2010.

[63] X. Duan, Y. Huang, Y. Cui, J. Wang, and C. M. Lieber, "Indium phosphide nanowires as building blocks for nanoscale electronic and optoelectronic devices," *Nature*, vol. 409, no. 6816, pp. 66–69, 2001.

[64] X. Duan, Y. Huang, R. Agarwal, and C. M. Lieber, "Single-nanowire elecctrically driven lasers," *Nature*, vol. 421, no. 6920, pp. 241–245, 2003.

[65] M. Law, D. J. Sirbuly, J. C. Johnson, J. Goldberger, R. J. Saykally, and P. Yang, "Nanoribbon waveguides for subwavelength photonics integration," *Science*, vol. 305, no. 5688, pp. 1269–1273, 2004.

[66] D. J. Sirbuly, M. Law, P. Pauzauskie et al., "Optical routing and sensing with nanowire assemblies," *Proceedings of the National Academy of Sciences of the United States of America*, vol. 102, no. 22, pp. 7800–7805, 2005.

[67] P. J. Pauzauskie and P. Yang, "Nanowire photonics," *Materials Today*, vol. 9, no. 10, pp. 36–45, 2006.

[68] L. J. Lauhon, M. S. Gudlksen, D. Wang, and C. M. Lieber, "Epitaxial core-shell and core-multishell nanowire heterostructures," *Nature*, vol. 420, no. 6911, pp. 57–61, 2002.